Thermal expansion of cancrinite

ISHMAEL HASSAN

Department of Geology, Faculty of Science, University of Kuwait, P.O. Box 5969, Safat, 13060, Kuwait

Abstract

Thermal expansion coefficients were measured for a cancrinite from Bancroft, Ontario, Canada. Measurements of cell parameters and unit-cell volumes were obtained at room temperature and at heating intervals of 50°C over the temperature range from 50 to 1400°C. The unit-cell parameters for cancrinite increase non-linearly with temperature up to 1200°C and shortly thereafter, the mineral melted. The *c* parameter increases more rapidly than the *a* parameter, and the *c/a* ratio increases linearly with temperature. A plausible thermal expansion mechanism for cancrinite, which is based on the framework expansion that occurs as a function of cavity content, is presented. In the thermal expansion of cancrinite, the short Na-H_2O in the H_2O–Na—H_2O chain expands to form equal distances to the two H_2O molecules in the chain. This causes the Na atoms to move towards the plane of the six-membered rings and forces the tetrahedra to rotate and the rings become more planar. The Na atoms then form bonds to all six (O1 and O2) oxygen atoms in a ring; the Na-O1 bonds become shorter and the Na-O2 bonds become longer. These effects cause an increase in both *a* and *c*, and thus an increase in the *c/a* ratio. A similar thermal expansion mechanism operates in the sodalite-group minerals where the six-membered rings and Na-Cl bond are involved.

KEYWORDS: cancrinite, cancrinite-group, thermal expansion, powder X-Ray diffraction.

Introduction

THE structures of the cancrinite-group minerals are characterized by parallel six-membered rings consisting of alternating AlO_4 and SiO_4 tetrahedra. The hexagonal symmetry is the result of the stacking of such six-membered rings in an AB... sequence. This stacking leads to large continuous channels that are formed by twelve-membered rings of alternating AlO_4 and SiO_4 tetrahedra (Fig. 1*a*). These are among the largest channels known for zeolites. The cancrinite structure also consists of small cages, known as ε-cages in zeolite chemistry. The ε-cage is also known as cancrinite cage or 'undecahedral' cage, which is bounded by 5 six-membered and 6 four-membered rings and, thus, the ε-cage is also known as 11-hedral cage (Fig. 1*b*). The ε-cages occur along the three-fold axes (Fig. 1*a*).

Crystal-chemical data for a few common members of the cancrinite group are given (Table 1). The stacking of six-membered rings in these cancrinites is the AB... sequence (Fig. 1*b*). In general, the ε-cages contain atoms or clusters of atoms that have a net charge difference of 1+ valence units. For example, $[Na{\cdot}H_2O]^+$ clusters occur in the ε-cages of cancrinite, hydroxy-cancrinite, and vishnevite, but $[Ca{\cdot}Cl]^+$ clusters occur in davyne. The ε-cage in microsommite contains an Na cation, while tiptopite, the beryllophosphate analogue of hydroxy (basic) cancrinite, contains a K cation (Table 1). The other interstitial cations and anions occur in the large channels that are parallel to the 6_3 axes (Fig. 1*a*). Microsommite has a *c* parameter that is similar to that of cancrinite. However, its unit cell is three times (Z = 3) that of cancrinite, with $a_m = \sqrt{3}\ a_c$. Other variations in the *a* cell parameter occur in pitiglianoite and quadridavyne (Table 1).

The sodalite-group minerals have strong structural similarities to the cancrinite-group minerals, but the former have an ABC... stacking sequence that leads to cubic instead of hexagonal symmetry. This sequence leads to an offset of the C-type layer and causes a network of large β-cages in the sodalite-group minerals.

Thermal expansion studies were made on many sodalite-group minerals and their structures were also modeled at elevated temperatures (e.g. Demsey and Taylor, 1980; Henderson and Taylor, 1978; Hassan and Grundy, 1984*a*, 1991*a*); however, similar studies were not done on cancrinite or other members of the

Mineralogical Magazine, December 1996, Vol. 60, pp. 949–956

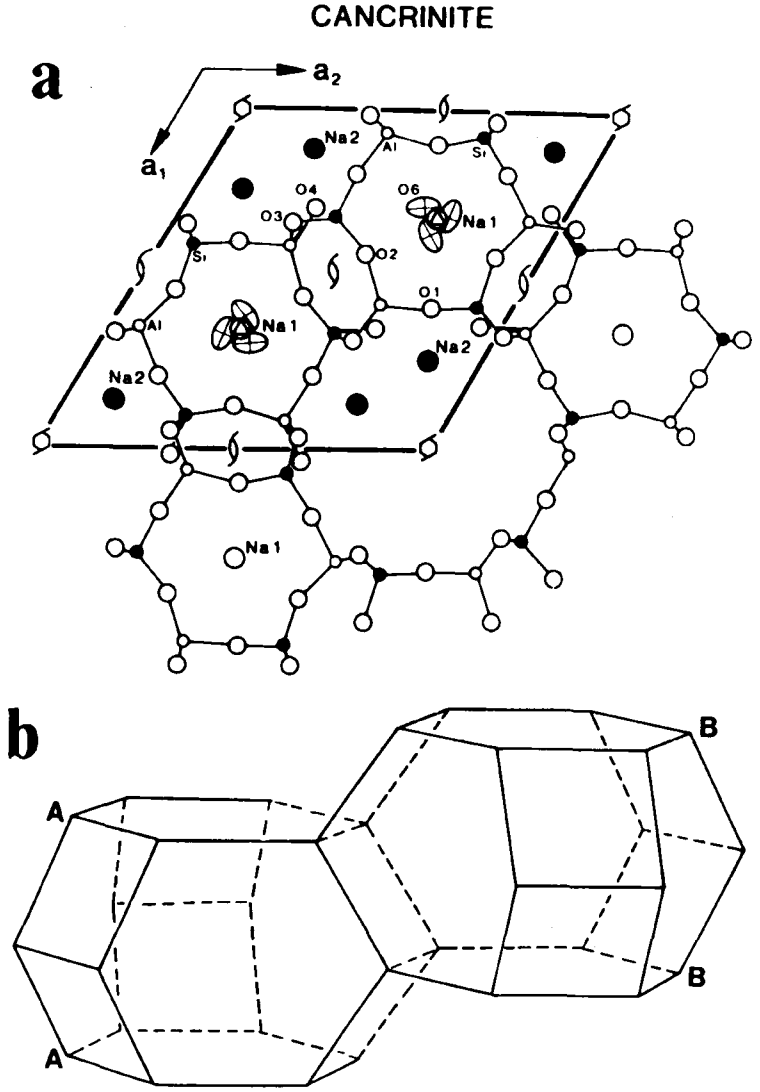

FIG. 1. (*a*) Crystal structure of cancrinite showing four-, six-, and twelve-membered rings of alternating SiO_4 and AlO_4 tetrahedra (after Grundy and Hassan, 1982). (*b*) Schematic illustration of the two ε-cages per unit cell in cancrinite.

cancrinite-group. This paper reports work carried out on cancrinite as part of an ongoing project to characterize these related mineral groups.

Experimental

Sample description. The specimen used in this study is from Dungannon Township, Ontario, Canada (McMaster University collection # 68024). The chemical composition is $Na_{5.96}Ca_{1.52}[Al_6Si_6O_{24}](CO_3)_{1.57}\cdot 1.75H_2O$, with hexagonal symmetry, unit-cell parameters of $a_o = 12.590$, $c_o = 5.117$ Å, and a hexagonal supercell with parameters of a_o by $8 \times c_o$ (= 40.936 Å; Grundy and Hassan, 1982).

A finely powdered sample of cancrinite was obtained by crushing fragments of the specimen

TABLE 1. Cancrinite-group minerals: formulae, ε-cage clusters, unit-cell parameters

Mineral	Chemical formula	ε-Cage Clusters	Cell (Å) *a*	Cell (Å) *c*	*c/a*	*V*(Å^3)	Space group	R%	Selected reference
Cancrinite	$Na_6Ca_2[Al_6Si_6O_{24}](CO_3)_2{\cdot}2H_2O$	$[Na{\cdot}H_2O]^+$	12.590	5.117	0.4060	702.4	$P6_3$	2.8	Grundy & Hassan (1982)
Hydroxy (basic) cancrinite	$Na_8[Al_6Si_6O_{24}](OH)_2{\cdot}3H_2O$	$[Na{\cdot}H_2O]^+$	12.664	5.159	0.4074	716.5	$P6_3$	4.7	Hassan & Grundy (1991*b*)
Vishnevite	$Na_{6.5}K_{0.4}[Al_6Si_6O_{24}](SO_4)_{0.5}{\cdot}2H_2O$	$[Na{\cdot}H_2O]$	12.685	5.179	0.4083	721.7	$P6_3$	3.7	Hassan & Grundy (1984*b*)
Pitiglianoite	$Na_6K_2[Al_6Si_6O_{24}]SO_4{\cdot}2H_2O$	$[Na{\cdot}H_2O]^+$	12.771*	5.221	0.4088	737.5	$P6_3/m$	6.5	Merlino *et al.* (1991)
Davyne-1	$Na_3K_{2.6}Ca_2[Al_6Si_6O_{24}](SO_4)_{0.5}Cl_2$	[Ca·Cl]*	12.793	5.367	0.4195	760.7	$P6_3$	4.8	Hassan & Grundy (1990)
Davyne-2	$Na_{4.4}K_{1.5}Ca_{2.1}[Al_6Si_6O_{24}](SO_4)_{0.6}Cl_{2.8}$	[Ca·Cl]*	12.705	5.368	0.4225	750.4	$P6_3/m$	4.9	Bonaccorsi *et al.* (1990)
Quadridavyne	$Na_{4.0}K_{1.4}Ca_{2.2}[Al_6Si_6O_{24}](SO_4)_{0.2}Cl_{3.76}$	[Ca·Cl]*	12.885‡	5.371	0.4168	772.2	$P6_3/m$	§	Bonaccorsi *et al.* (1994)
Microsommite	$Na_{5.7}K_{2.3}[Al_6Si_6O_{24}](SO_4)_{1.0}$	$[Na]^+$	12.729†	5.237	0.4094	742.2	$P6_3$	–	See Merlino (1984)
Tiptopite	$K_2Li_{2.9}Na_{1.7}Ca_{0.7}[Be_6P_6O_{24}](OH)_2{\cdot}1.33H_2O$	$[K]^+$	11.655	4.962	0.4257	583.7	$P6_3$	7.9	Peacor *et al.* (1987)

* Recalculated parameter for cancrinite cell; c = cancrinite; m = microsommite; qd = quadridavyne; p = pitiglianoite; † $a_c = a_m/\sqrt{3}$; ‡ $a_c = \frac{1}{2}a_{qd}$; * $a_c = a_p/\sqrt{3}$. § Only preliminary structural data are available.

using an agate mortar and pestle. The powdered sample was pressed into the sample holder and diffraction data were obtained at various temperatures.

High-temperature powder X-ray diffraction measurements. Powder X-ray diffraction data for cancrinite were obtained in the Department of Geology with a recently acquired, fully computerized, Siemens D5000 Diffractometer. The high-temperature X-ray diffraction data were obtained in a high vacuum ($<10^{-6}$ mbar) using a water-cooled Buhler's HDK S1 Chamber producing temperatures ranging from 20 to 1600°C. The diffractometer was set up in the θ-θ operating mode. The sample was heated using a computer controlled REP 1800 heating unit consisting of a high-current transformer (8.5 V, 100 A). This unit is operated with two sets of control parameters for optimal temperature control. A thin metal strip (50 × 8 × 0.1 mm) with a small cup-like depression is clamped over two electrodes and this strip serves as both sample carrier and heater at the same time. The sample carrier is stretched by means of a turnable electrode and a spring for automatic compensation of its thermal expansion at high temperatures. The sample strip is made of PtRh. In the HDK S1, Pt10%Rh-Pt (EL10) thermocouples are used. At one side, the welding beads of the EL 10 thermocouples are spot-welded to the back of the sample carrier and the remaining lengths are isolated by small tubules made of Al_2O_3 and the other ends are attached to the thermocouple feed through *via* Cu connecting pins that have small holes through which the thermocouple wires are inserted. A small soldering iron and a little soft solder are used to make a good connection. A small amount of fine-grained powder is placed in the cup-like depression of the sample carrier and a Ni heat shield is placed over the sample carrier. The thickness of the powder layer is approximately 0.2 mm.

High-temperature X-ray diffraction data were obtained with the diffractometer operating in the vertical position and in the θ-θ operating mode. Monochromatic Cu-$K\alpha_1$ radiation, obtained with an incident beam monochromator, was used in conjunction with a scintillation counter. Data were collected in the 2θ range of 15 to 40°. A continuous scan was used with a step size of 0.04° and step time of 2.0 s. The computer was programmed to collect data at 20°C, 50°C and thereafter in intervals of 50°C to a maximum temperature of 1400°C. The heating rate was 1°C/s and a delay of 30 s was set before data collection began at each successive temperature.

The unit-cell parameters for cancrinite were determined at the different temperatures by least-squares refinement using the commercial program WIN METRIC.

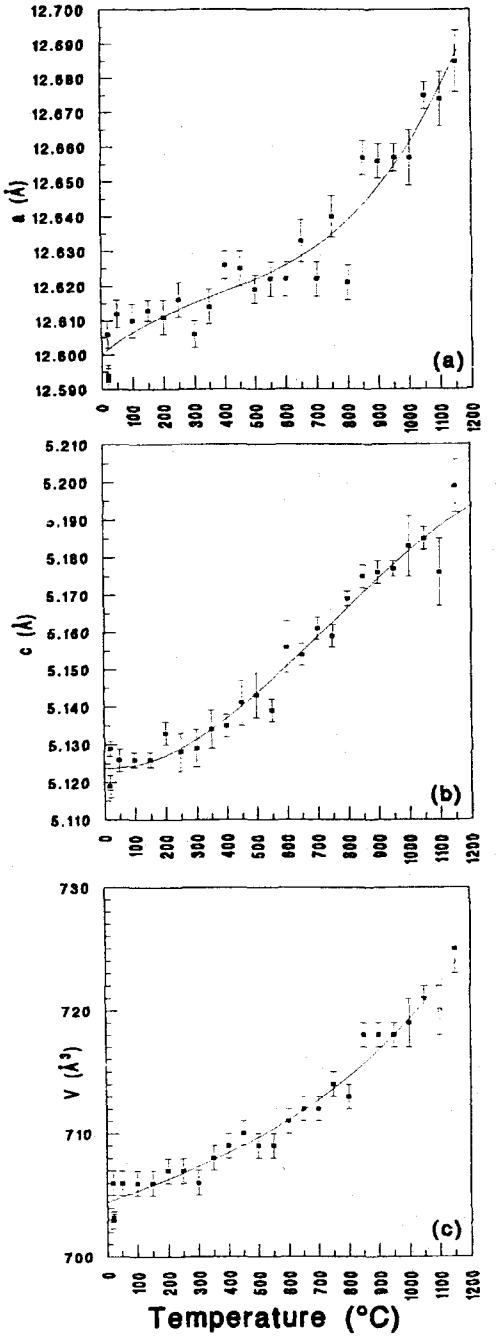

FIG. 2. The variation of the unit-cell parameters with temperature for cancrinite. (*a*) *a vs. T*, (*b*) *c vs. T*, and (*c*) *V vs. T*. The unit-cell parameters increase non-linearly with temperature.

TABLE 2. Cancrinite unit-cell parameters at different temperatures from 20 to 1150°C

Temp T (°C)	Cell parameters a (Å)	$(\Delta a/a_o)100$	c (Å)	$(\Delta c/c_o)100$	V (Å^3)	$(\Delta V/V_o)100$
20†	12.594(2)	0.000	5.119(1)	0.000	703.2(3)	0.000
20‡	12.593(4)	0.000	5.119(3)	0.000	703.0(7)	0.000
20	12.60 6(4)	0.095	5.129(2)	0.195	706(1)	0.398
50	12.612(4)	0.143	5.126(3)	0.137	706(1)	0.398
100	12.610(5)	0.127	5.126(2)	0.137	706(1)	0.398
150	12.613(3)	0.151	5.126(2)	0.137	706(1)	0.398
200	12.611(5)	0.135	5.133(3)	0.273	707(1)	0.540
250	12.616(5)	0.175	5.128(5)	0.176	707(1)	0.540
300	12.606(4)	0.095	5.129(5)	0.195	706(1)	0.398
350	12.614(5)	0.159	5.134(5)	0.293	708(1)	0.683
400	12.626(4)	0.254	5.135(3)	0.313	709(1)	0.825
450	12.625(5)	0.246	5.141(6)	0.430	710(1)	0.967
500	12.619(4)	0.199	5.143(6)	0.469	709(1)	0.825
550	12.622(5)	0.222	5.139(3)	0.391	709(1)	0.825
600	12.622(5)	0.222	5.156(7)	0.723	711(1)	1.109
650	12.633(6)	0.310	5.154(3)	0.684	712(1)	1.251
700	12.622(5)	0.222	5.161(3)	0.820	712(1)	1.251
750	12.640(6)	0.365	5.159(3)	0.781	714(1)	1.536
800	12.621(5)	0.214	5.169(2)	0.977	713(1)	1.394
850	12.657(5)	0.500	5.175(3)	1.094	718(1)	2.105
900	12.656(5)	0.492	5.176(3)	1.113	718(1)	2.105
950	12.657(4)	0.500	5.177(2)	1.133	718(1)	2.105
1000	12.657(8)	0.500	5.183(8)	1.250	719(2)	2.247
1050	12.675(4)	0.643	5.185(3)	1.289	721(1)	2.531
1100	12.674(8)	0.635	5.176(9)	1.113	720(2)	2.389
1150	12.685(9)	0.723	5.199(7)	1.563	725(2)	3.100

† 2θ range is 10 to 110°; θ-2θ mode; Cu-$K\alpha$1 radiation, step size = 0.02°; step time = 10s.
‡ 2θ range is 15 to 40° and is extracted from the above data set.

Results and discussion

The refined unit-cell parameters are given in Table 2 and displayed graphically in Figs 2 and 3. The unit-cell parameters increase non-linearly with increasing temperature (Figs 2 and 3). There are changes or discontinuities in the thermal expansion curves that indicate changes in the material as it is heated (e.g. loss of H_2O, CO_2, etc.). These changes, however, are best considered elsewhere in conjunction with differential thermal analyses (DTA, TG, etc.; see Hassan, 1996). At 1200°C, the diffraction peaks were becoming weak and the sample melted shortly above 1200°C, but below 1250°C. The variation of unit-cell parameters and the percentage changes of unit-cell parameters with temperature were fitted to polynomials using least-squares refinement (Table 3). The c parameter increases more than the a parameter (Fig. 3), but the c/a ratio increases linearly with temperature (Fig. 4). The c/a ratios for the cancrinite-group minerals (Table 1) are shown for comparison in Fig. 4.

High-temperature structural data are not available for cancrinite-group minerals. Therefore, it is difficult to formulate an exact mechanism of thermal expansion for cancrinite. However, such a mechanism can be deduced if changes in chemistry cause changes in cell parameters, which are analogous to those of thermal expansion.

In considering the channel ions, the increase in the c/a ratio is for minerals containing CO_3 (cancrinite), to OH (hydroxy cancrinite), to SO_4 with minor K (vishnevite, pitiglianoite, microsommite), to K with minor SO_4 (davyne-1, 2 and quadridavyne). Thus, the increase in c/a follows the increase in size of the channel anions. The CO_3 anion is planar; OH anions occupy the same positions as the oxygens of the CO_3 group, and the SO_4 group has a tetrahedral shape. The basal oxygen atoms of the SO_4 group occupy the same positions as the oxygens of the planar CO_3 group. The K cation seems to have the most significant effect on the c/a ratio, followed by SO_4, OH, and

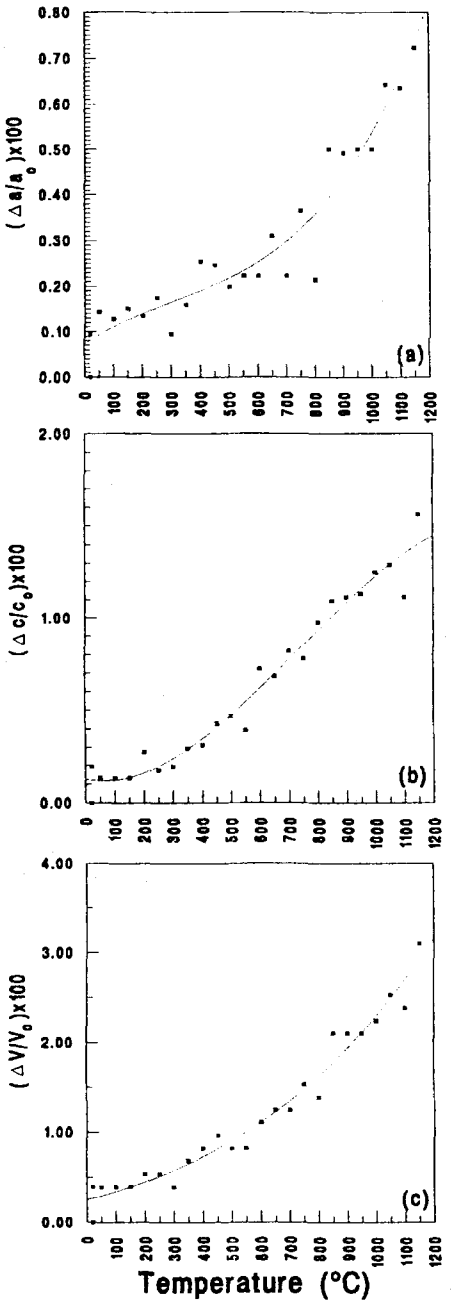

FIG. 3. The variation of the percentage changes in unit-cell parameters with temperature for cancrinite. (*a*) $\Delta a/a_o$ *vs. T*, (*b*) $\Delta c/c_o$ *vs. T*, and (*c*) $\Delta V/V_o$ *vs. T*. The unit-cell parameters increase non-linearly with temperature. With increasing temperature, the *c* parameter increases more rapidly than the *a* parameter.

CO_3 in decreasing significance among the minerals, excluding davyne (Fig. 4).

The cages in davyne-1, davyne-2, and quadridavyne contain $[Ca{\cdot}Cl]^+$ clusters, and they have the largest *c/a* ratios for the aluminosilicate cancrinites (Table 1, Fig. 4). In contrast, $[Na{\cdot}H_2O]^+$ clusters occur in cancrinite, hydroxy cancrinite, vishnevite, and pitiglianoite and they have the smallest *c/a* ratios. The latter group of minerals have similar values for *c* and *a*, but those for davyne group are significantly larger (Table 1; Fig. 4). The increase in cell parameters for the davyne group seems to result from the increase in size of the cages that arise from the substitution of $[Ca{\cdot}Cl]^+$ for $[Na{\cdot}H_2O]^+$. This substitution causes a larger increase in *c* compared with *a*; thus davyne has the largest *c/a* value at room temperature compared with the other members of the aluminosilicate cancrinite group, and davyne also has the largest cell volume (Table 1). The microsommite cage contains $[Na]^+$, and so its recalculated *c/a* ratio

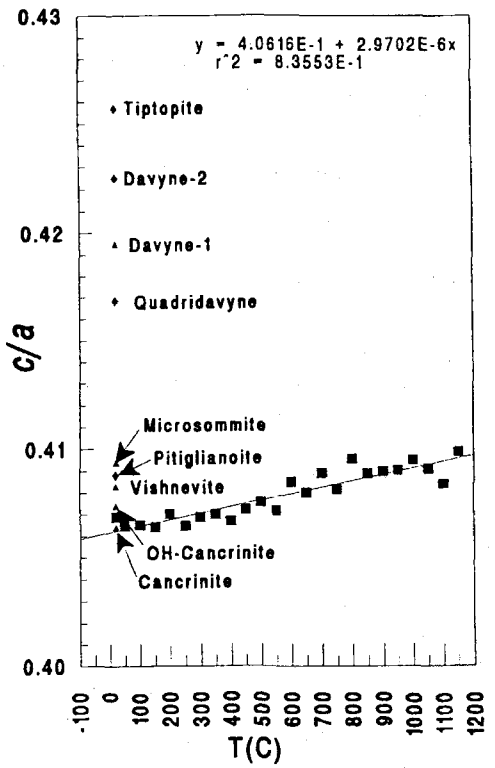

FIG. 4. Linear increase of the *c/a* ratio with temperature for cancrinite. The *c/a* ratios for the cancrinite-group minerals (Table 1) are shown for comparison. Insert is the equation of the least-squares fit to the data for cancrinite.

TABLE 3. Least-squares fit to the variation of the unit-cell parameters with temperature

a	= 12.600	$+7.2872 \times 10^{-5}T$	$-1.0646 \times 10^{-7}T^2$	$+9.4778 \times 10^{-11}T^3$	$r^2 = 0.923$
c	= 5.1239	$-4.6607 \times 10^{-6}T$	$+1.1321 \times 10^{-7}T^2$	$-5.0752 \times 10^{-11}T^3$	$r^2 = 0.966$
V	= 704.44	$+9.3443 \times 10^{-3}T$	$-1.1698 \times 10^{-6}T^2$	$+6.7094 \times 10^{-9}T^3$	$r^2 = 0.966$
$\Delta a/a_o$	= 0.072349	$+4.3507 \times 10^{-4}T$	$-6.0532 \times 10^{-7}T^2$	$+6.3481 \times 10^{-10}T^3$	$r^2 = 0.923$
$\Delta c/c_o$	= 0.12772	$-2.8988 \times 10^{-4}T$	$+2.5439 \times 10^{-6}T^2$	$-1.1548 \times 10^{-9}T^3$	$r^2 = 0.966$
$\Delta V/V_o$	= 0.25553	$+8.4185 \times 10^{-4}T$	$+6.4788 \times 10^{-7}T^2$	$+5.5398 \times 10^{-10}T^3$	$r^2 = 0.967$

might be expected to be smaller than for cancrinite-group minerals whose cages contain $[Na{\cdot}H_2O]^+$ clusters, but this effect is not observed.

Consideration of the coordinations of the cage clusters gives some insight into the thermal expansion mechanism in cancrinite-group minerals (Table 4, Fig. 1). Among the minerals that contain $[Na{\cdot}H_2O]^+$ clusters, cancrinite has the smallest *c/a* ratio followed by hydroxy cancrinite, vishnevite, and pitiglianoite, respectively. This trend parallels the increase in size of the mean bond-length for 8-coordinated Na (Table 4), which occurs on the Na1 site. The davyne-group minerals have the largest *c/a* ratio, but the shortest mean bond-length for 8-coordinated Ca compared with 8-coordinated Na (Table 4).

The Na–O1 bonds in these minerals are longer than the Na–O2 bonds (Table 4). In davynes, the Ca–O1 bonds are shorter than the Na-O1 bonds in the above minerals, but the Ca-O2 bonds are longer than the Na-O2 bonds. In the H_2O–Na—H_2O linear coordination, the Na is closer to one H_2O molecule than the other, but in the Cl–Ca–Cl linear coordination, the Ca in mid-way between the two Cl's. Therefore, in replacing $[Na{\cdot}H_2O]^+$ by $[Ca{\cdot}Cl]^+$ clusters, the Ca atoms move towards the centre of the six-membered rings that cap the cages and force the tetrahedra to rotate and the rings become more planar. These effects cause an increase in both the *a* and *c* dimensions of the cell and thus cause an increase in the *c/a* ratio. The thermal expansion mechanism for cancrinite follows a similar path.

By analogy with the framework expansion that occurs as a function of cavity content, it might be suggested that in the thermal expansion of cancrinite, the short Na–H_2O in the H_2O–Na—H_2O chain expands to form equal distances to the two H_2O molecules in the chain. This causes the Na atoms to move towards the plane of the six-membered rings and force the tetrahedra to rotate and the rings become more planar. The Na atoms then form bonds to all six O1 and O2 oxygen atoms (Fig. 1); the Na–O1 bonds become shorter and the Na–O2 bonds become longer. These effects cause an increase in both *a* and *c*, and thus a linear increase in the *c/a* ratio, as observed (Fig. 4). A similar thermal expansion mechanism operates in the sodalite-group minerals where the six-membered rings and Na-Cl bond are involved (see Hassan and Grundy, 1984*a*).

Acknowledgements

An anonymous referee is thanked for useful comments on this paper. This work was financially supported by the University of Kuwait in the form of a Research Grant (SG-038). The X-ray diffraction measurements were made in the Department of Geology, University of Kuwait.

References

Bonaccorsi, E., Merlino, S. and Pasero, M. (1990) Davyne: its structural relationships with cancrinite and vishnevite. *Neues Jahrb. Mineral. Mh.*, **3**, 97–112.

Bonaccorsi, E., Merlino, S., Orlandi, P., Pasero, M. and Vezzalini, G. (1994) Quadridavyne, $[(Na,K)_6Cl_2][Ca_2Cl_2][Al_6Si_6O_{24}]I_2$, a new feld-

TABLE 4. Comparison of the coordinations of the cage clusters

Bonds	Davyne-1	Davyne-2	Bonds	Cancrinite	OH-Cancrinite	Vishnevite	Pitiglianoite
Ca–O1 ×3	2.659 Å	2.596 Å	Na–O1 ×3	2.86 3 Å	2.894 Å	2.884 Å	2.930 Å
–O2 ×3	2.538	2.566	–O2 ×3	2.450	2.417	2.429	2.398
–Cl ×1	2.664	2.704	–H_2O ×1	2.335	2.369	2.330	2.330
–Cl ×1	2.702	2.704	–H_2O ×1	2.874	2.899	2.960	3.010
Mean for [8]	2.619	2.612	Mean for [8]	2.644	2.650	2.654	2.666

spathoid mineral from Vesuvius area. *Eur. J. Mineral.*, **6**, 481–7.

Demsey, M.J. and Taylor, D. (1980) Distance least squares modelling of the cubic sodalite structure and the thermal expansion of $Na_8[Al_6Si_6O_{24}]I_2$. *Phys. Chem. Mineral.*, **6**, 197–208.

Grundy, H.D. and Hassan, I. (1982) The crystal structure of a carbonate-rich cancrinite. *Canad. Mineral.*, **20**, 239–51.

Hassan, I. (1996) The thermal behaviour of cancrinite. *Canad. Mineral.*, **34** (in press).

Hassan, I. and Grundy, H.D. (1984*a*) The crystal structures of sodalite-group minerals. *Acta Crystallogr.*, **B40**, 6–13.

Hassan, I. and Grundy, H.D. (1984*b*) The character of the cancrinite-vishnevite solid-solution series. *Canad. Mineral.*, **22**, 333–40.

Hassan, I. and Grundy, H.D. (1990) The structure of davyne and implications for stacking faults. *Canad. Mineral.*, **28**, 341–9.

Hassan, I. and Grundy, H.D. ((1991*a*) The crystal structure and thermal expansion of tugtupite, $Na_8[Al_2Be_2Si_8O_{24}]Cl_2$. *Canad. Mineral.*, **29**, 385–90.

Hassan, I. and Grundy, H.D. ((1991*b*) The crystal structure of basic cancrinite, ideally $Na_8[Al_6Si_6O_{24}]\cdot 3H_2O$. *Canad. Mineral.*, **29**, 377–84.

Henderson, C.M.B. and Taylor, D. (1978) The thermal expansion of synthetic aluminosilicate-sodalites, $M_8[Al_6Si_6O_{24}]X_2$. *Phys. Chem. Mineral.*, **2**, 337–47.

Merlino, S. (1984) Feldspathoids: their average and real structures. *NATO ASI C*, **137**, 435–70.

Merlino, S., Mellini, M., Bonaccorsi, E., Pasero, M., Leoni, L. and Orlandi, P. (1991) Pitiglianoite, a new feldspathoid from southern Tuscany, Italy: chemical composition and crystal structure. *Amer. Mineral.*, **76**, 2003–8.

Peacor, D.R., Rouse, R.C., and Ahn, J-H. (1987) Crystal structure of tiptopite, a framework beryllophosphate isotypic with basic cancrinite. *Amer. Mineral.*, **72**, 816–20.

[*Manuscript received 14 November 1995: revised 29 April 1996*]